Retinal Structure and Function in Achromatopsia

Implications for Gene Therapy

Venki Sundaram, FRCOphth,[1,2] Caroline Wilde, MBBS,[1] Jonathan Aboshiha, FRCOphth,[1,2] Jill Cowing, PhD,[1] Colin Han,[3] Christopher S. Langlo,[4] Ravinder Chana, MSc,[1,2] Alice E. Davidson, PhD,[1,2] Panagiotis I. Sergouniotis, MD, PhD,[1] James W. Bainbridge, PhD, FRCOphth,[1,2] Robin R. Ali, PhD,[1] Alfredo Dubra, PhD,[5,6] Gary Rubin, PhD,[1] Andrew R. Webster, MD, FRCOphth,[1,2] Anthony T. Moore, FRCOphth,[1,2] Marko Nardini, PhD,[1] Joseph Carroll, PhD,[4,5,6] Michel Michaelides, MD, FRCOphth[1,2]

Purpose: To characterize retinal structure and function in achromatopsia (ACHM) in preparation for clinical trials of gene therapy.

Design: Cross-sectional study.

Participants: Forty subjects with ACHM.

Methods: All subjects underwent spectral domain optical coherence tomography (SD-OCT), microperimetry, and molecular genetic testing. Foveal structure on SD-OCT was graded into 5 distinct categories: (1) continuous inner segment ellipsoid (ISe), (2) ISe disruption, (3) ISe absence, (4) presence of a hyporeflective zone (HRZ), and (5) outer retinal atrophy including retinal pigment epithelial loss. Foveal and outer nuclear layer (ONL) thickness was measured and presence of hypoplasia determined.

Main Outcome Measures: Photoreceptor appearance on SD-OCT imaging, foveal and ONL thickness, presence of foveal hypoplasia, retinal sensitivity and fixation stability, and association of these parameters with age and genotype.

Results: Forty subjects with a mean age of 24.9 years (range, 6–52 years) were included. Disease-causing variants were found in *CNGA3* (n = 18), *CNGB3* (n = 15), *GNAT2* (n = 4), and *PDE6C* (n = 1). No variants were found in 2 individuals. In all, 22.5% of subjects had a continuous ISe layer at the fovea, 27.5% had ISe disruption, 20% had an absent ISe layer, 22.5% had an HRZ, and 7.5% had outer retinal atrophy. No significant differences in age ($P = 0.77$), mean retinal sensitivity ($P = 0.21$), or fixation stability ($P = 0.34$) across the 5 SD-OCT categories were evident. No correlation was found between age and foveal thickness ($P = 0.84$) or between age and foveal ONL thickness ($P = 0.12$).

Conclusions: The lack of a clear association of disruption of retinal structure or function in ACHM with age suggests that the window of opportunity for intervention by gene therapy is wider in some individuals than previously indicated. Therefore, the potential benefit for a given subject is likely to be better predicted by specific measurement of photoreceptor structure rather than simply by age. The ability to directly assess cone photoreceptor preservation with SD-OCT and/or adaptive optics imaging is likely to prove invaluable in selecting subjects for future trials and measuring the trials' impact. *Ophthalmology 2014;121:234-245 © 2014 by the American Academy of Ophthalmology.*

Achromatopsia (ACHM) is a cone dysfunction syndrome with an incidence of approximately 1 in 30 000, which presents at birth or early infancy.[1] It is characterized by marked photophobia and nystagmus, reduced visual acuity (20/120 to 20/200), very poor or absent color vision, and absent cone electroretinogram responses, with normal rod function. Fundus examination is usually normal, although retinal pigment epithelial (RPE) disturbance and atrophy may be present. Mutations in 5 genes have been identified in ACHM: *CNGA3*, *CNGB3, GNAT2, PDE6C*, and *PDE6H*, all of which encode components of the cone phototransduction cascade.[2–5] *CNGA3* and *CNGB3* encode the α and β subunits of the cGMP-gated cation channel, respectively, and account for approximately 80% of cases of ACHM.[1,2] Sequence variants in *GNAT2, PDE6C*, and *PDE6H* are uncommon causes of ACHM, each accounting for <2% of patients, and encode the α-subunit of transducin and the α and γ subunits of cGMP phosphodiesterase, respectively.[3–5]

There have been several optical coherence tomography (OCT)–based studies that have investigated outer retinal

ISSN 0161-6420/14/$ - see front matter
http://dx.doi.org/10.1016/j.ophtha.2013.08.017

architecture and foveal morphology in ACHM.[6–9] The macular appearances described include normal lamination, variable degrees of disruption of the hyperreflective photoreceptor bands (known as either the inner segment/outer segment [OS] junction or inner segment ellipsoid [ISe]), an optically empty cavity or hyporeflective zone (HRZ), and complete outer retinal and RPE loss.[6–9] There are significant limitations to these studies, including the fact that subjects were not genotyped in all cases, and many relied on qualitative metrics to analyze the OCT images. In addition, there are conflicting data on progression and the presence or absence of age-dependent outer retinal loss, with Thiadens et al[6] and Thomas et al[7] suggesting age-associated progression, whereas Genead et al[8] provided evidence that cone loss is not age dependent. These inconsistencies, and the fact that several groups around the world are in preparation for gene replacement clinical trials, makes it critical to elucidate the progressive nature (and thus the therapeutic window) in ACHM in a genotype-dependent fashion.

Several studies have shown that gene therapy can be effective in restoring cone function in multiple animal models of ACHM.[10–14] In a *Cngb3*$^{-/-}$ mouse model, subretinal gene delivery resulted in restoration of electrophysiologic function to near normal levels and significantly improved visual behavior,[13] with larger canine models of *CNGB3*-associated disease also showing increased electrophysiologic responses and improvements in navigational ability after gene replacement therapy.[14] In anticipation of the imminent human gene therapy trials for ACHM, we sought to characterize the relationship between retinal structure and function in a large number of molecularly proven subjects. This information is important to help identify the most suitable candidates for therapy, to determine the optimal timing for intervention, and to measure its impact using appropriate outcome measures.

Methods

Subjects

Forty subjects with a clinical diagnosis of ACHM were included in this study. Ten additional subjects with normal vision were recruited. The protocol of the study adhered to the tenets of the Declaration of Helsinki, was approved by the local Ethics Committees of Moorfields Eye Hospital and the Medical College of Wisconsin, and was performed with the informed consent of all subjects.

Clinical Assessments

All subjects underwent a clinical history and detailed ocular examination, including best-corrected visual acuity (BCVA) using an Early Treatment Diabetic Retinopathy Study chart, reading acuity using the MNRead chart, contrast sensitivity assessment using the Pelli-Robson chart at 1 m, color vision testing (Ishihara and Hardy Rand Rittler pseudoisochromatic plates), color fundus photography, spectral domain OCT (SD-OCT), and microperimetry (MP).

On the basis of their fundus appearance on color fundus photography, each subject was assigned to 1 of 3 categories: (1) no RPE disturbance, (2) RPE disturbance, or (3) atrophy.

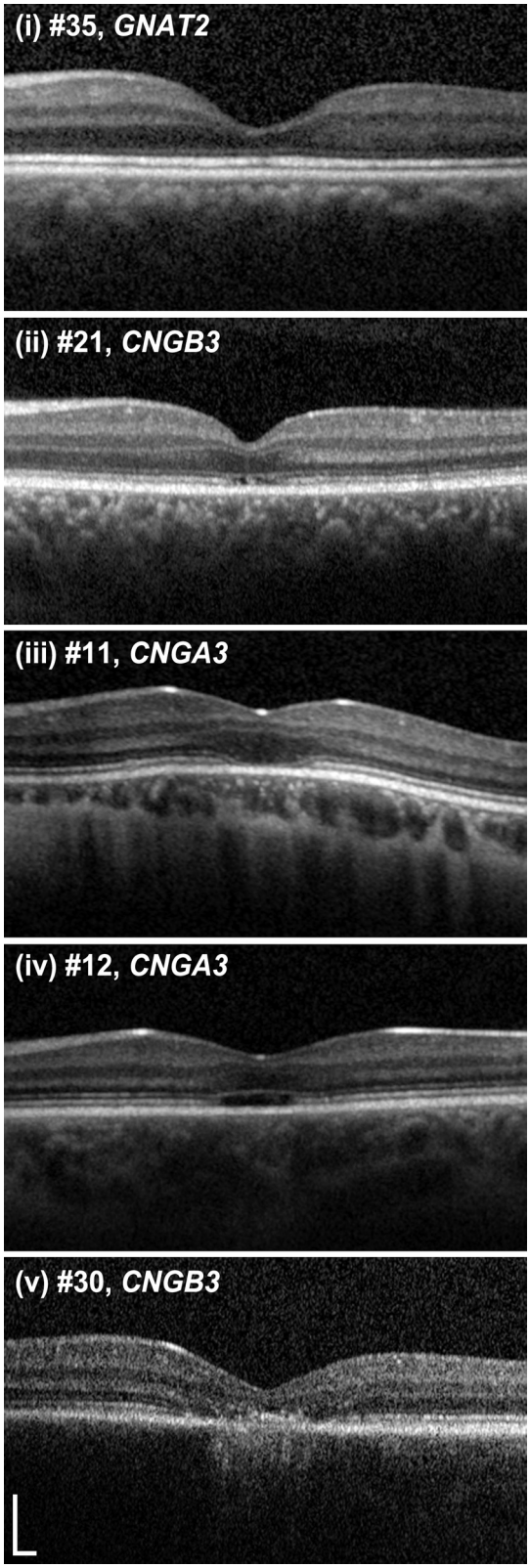

Figure 1. Representative images of the 5 optical coherence tomography phenotypes. Subjects were graded into 1 of 5 categories: (i) continuous inner segment ellipsoid (ISe) band, (ii) ISe disruption, (iii) ISe absence, (iv) hyporeflective zone present, and (v) outer retinal atrophy. Scale bar, 200 μm.

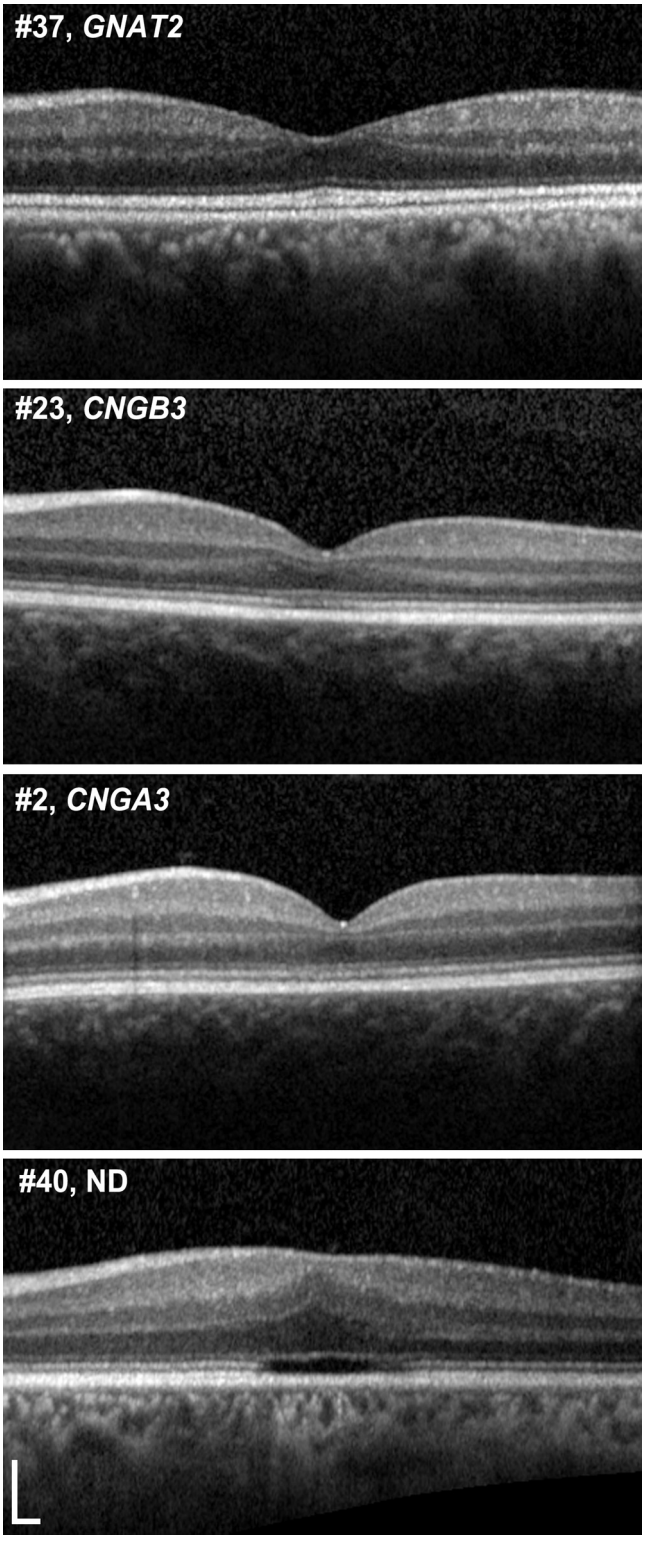

Figure 2. Representative examples of varying degrees of foveal hypoplasia. Foveal hypoplasia was defined here as the persistence of ≥1 inner retinal layers (outer plexiform layer, inner nuclear layer, inner plexiform layer, or ganglion cell layer) through the foveal center. Normal retinal anatomy (top panel) shows complete excavation of the inner retinal layers at the fovea, resulting in the characteristic "pit." However, in a number of conditions (such as retinopathy of prematurity and albinism), this process is impaired ("foveal hypoplasia"), resulting in retinas in which the inner retinal layers persist at the fovea. Interestingly, this can also be seen in achromatopsia. The 3 lower panels show examples of varying degrees of foveal hypoplasia in patients with achromatopsia, in whom the fovea contains inner retinal layers as opposed to complete excavation of these layers. Twenty-one of the 40 subjects (52.5%) had foveal hypoplasia, although it was not possible to assess hypoplasia in 2 subjects because of severe foveal atrophy. There was no difference in age, contrast sensitivity, retinal sensitivity, or fixation stability between subjects with or without foveal hypoplasia (see text). Scale bar, 200 μm. ND = no data.

SD-OCT

For all subjects (80 eyes of 40 subjects), after pupillary dilation, line and volume scans were obtained using a Spectralis SD-OCT (Heidelberg Engineering, Heidelberg, Germany). The volume acquisition protocol consisted of 49 B-scans (124 μm between scans; 20×20°), with Automatic Real Time eye tracking used when possible. The lateral scale of each image was estimated using the axial length data obtained from the Zeiss IOL Master (Carl Zeiss Meditec, Jena Germany).

Qualitative Assessment of Foveal Morphology. Foveal structure on SD-OCT images was graded into 1 of 5 categories (Fig 1): (1) continuous ISe, (2) ISe disruption, (3) ISe absence, (4) presence of an HRZ, or (5) outer retinal atrophy, including RPE loss. The presence/absence of foveal hypoplasia was also noted, defined as the persistence of ≥1 inner retinal layers (outer plexiform layer, inner nuclear layer, inner plexiform layer, or ganglion cell layer) through the fovea. Figure 2 shows examples of the varying degrees of foveal hypoplasia observed in the subjects examined herein. Consensus grading was established by 3 independent examiners (V.S., J.C., and M.M.).

Quantitative Analysis of Photoreceptor Structure on SD-OCT. We used a method that was conceptually similar to that described by Hood et al[15] to analyze the intensity of the ISe and external limiting membrane (ELM) bands, although there are a number of differences. First, our images were transformed into a linear display using a transform provided by the manufacturer. This is a critical correction to apply, because the native visualization of SD-OCT images on a logarithmic scale misrepresents the real differences in reflectivity (Fig 3). Second, we assessed layer intensity at only 2 specific retinal locations, 1 and 1.5 mm temporal to the fovea (because of the outer retinal disruption in many subjects, 1 mm was the closest eccentricity we could measure in all subjects). Finally, the procedure used to measure layer intensity was different. We generated longitudinal reflectivity profiles[16] at the 1- and 1.5-mm locations, and each longitudinal reflectivity profile was 5 pixels in width (Fig 3). Hood et al[15] defined a "local region" surrounding a specific segment of the ISe as extending ±275 μm to either side of the ISe segment and extending axially between the Bruch's membrane/choroid interface and the posterior border of the retinal nerve fiber layer.[15] Because other posterior layers may be altered because of the disruption in cone structure, including the outer nuclear layer (ONL) and Henle fiber layer, or the layers posterior to the ISe that are thought to originate from interactions between the photoreceptors and RPE,[17] we used a "local region" restricted to the retinal ganglion cell layer and inner plexiform layer. This is indicated by the horizontal arrows in Figure 3. We then measured the peak image intensity at the ELM and ISe (labeled in Fig 3), and the relative intensity of the ISe (or ELM) was taken as the ISe (or ELM) peak intensity divided by the average intensity in the "local region," generating the ISe (or ELM) intensity ratio used for analysis.

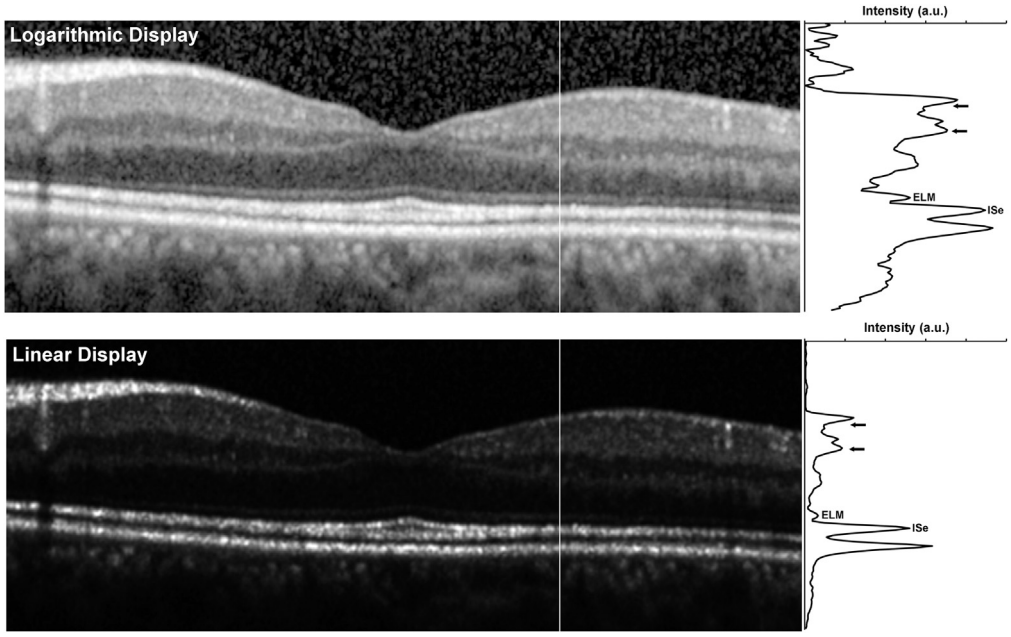

Figure 3. Longitudinal reflectivity profile assessment of photoreceptor integrity on spectral domain optical coherence tomography (SD-OCT). The top image is the native display of the image from the SD-OCT, whereas the lower image is a linear display of the actual image intensity. Note that in the linear (raw) SD-OCT image, greater differences in layer intensity get compressed when visualized on a logarithmic display. Moreover, the logarithmic transform will increase the widths of the hyperreflective bands being measured.[17] This highlights the need to use raw SD-OCT data when making quantitative measures of layer intensity. Vertical lines in each image indicate the location of the longitudinal reflectivity profile (LRP) shown to the right of each image. Short horizontal arrows define the boundaries of the "local region" used to normalize the inner segment ellipsoid (ISe) or external limiting membrane (ELM) intensity. a.u. = arbitrary units.

In addition to examining the ELM and inner segment/OS intensity, we measured the total retinal thickness (internal limiting membrane to RPE distance) and ONL thickness (ILM to ELM distance) at the fovea. In cases of foveal hypoplasia, the distance between the posterior outer plexiform layer boundary and the ELM was taken as the ONL thickness. All thickness measurements were conducted by a single observer (C.H.) using ImageJ software (National Institutes of Health, Bethesda, MD).

Microperimetry

MP was performed on both eyes of all subjects using the MP-1 microperimeter (Nidek Technologies, Padova, Italy). Specific details can be found in the online only material (Appendix 1, available at http://aaojournal.org). Fixation stability was assessed using the bivariate contour ellipse area (BCEA) which represents an area in degrees where 68% of fixation points are located;[18] this value is reported by the Nidek software.

Molecular Genetic Testing

Conventional direct Sanger sequencing of exons and exon-intron boundaries of *CNGA3*, *CNGB3, GNAT2*, and *PDE6C* was undertaken using previously published methods.[2–4] Subjects 39 and 40 also underwent screening of exons and exon-intron boundaries of *PDE6H*.[5]

Statistical Analysis

Normality of data was assessed by evaluating the shape of histogram plots, with age, BCVA, contrast sensitivity, and reading acuity considered to be normally distributed. Intereye correlations for all parameters were assessed using Pearson or Spearman correlation analysis where appropriate. The left eye was arbitrarily selected for further analysis, and differences in parameters between SD-OCT categories, fundus appearance category, and genotype were assessed using 1-way analysis of variance or the Kruskal-Wallis test where appropriate. Differences in parameters between subjects with or without foveal hypoplasia were assessed using either an independent samples *t*-test or Mann–Whitney *U* test where appropriate.

Results

Twenty male and 20 female subjects with a mean age of 24.9 years (range, 6–52 years) were included (Tables 1 and 2). Mean BCVA was 0.92 logarithm of the minimum angle of resolution (range, 0.72–1.32), mean contrast sensitivity was 1.16 logCS (range, 0.50–1.55), and mean reading acuity was 0.76 logarithm minimum angle of resolution (range, 0.5–1.32; Table 2). There was no correlation between age and (1) BCVA ($r = 0.18$; $P = 0.27$; Fig 4), (2) contrast sensitivity ($r = -0.27$; $P = 0.09$), or (3) reading acuity ($r = 0.29$; $P = 0.07$).

All subjects were able to read the Ishihara test plate, but were unable to read any subsequent plates or to correctly identify any of the Hardy Rand Rittler test plates.

Fundus examination revealed no evidence of macular RPE disturbance in 11 subjects (mean age, 19.5 years; range, 6–33 years) RPE disturbance in 20 subjects (mean age, 27.5 years; range, 12–52 years), and well-circumscribed macular atrophy in 9 subjects (mean age, 25.9 years; range, 11–43 years; Table 2). There was no difference in mean age, BCVA, contrast sensitivity, reading acuity, retinal sensitivity, or bivariate contour ellipse area between these 3 groups (Table 3, available at http://aaojournal.org).

Table 1. Summary of Retinal Structure Assessed with Spectral Domain-Optical Coherence Tomography in 40 Patients with Achromatopsia

Pt No.	Age (yr)	Sex	Axial Length (mm)	Gene	Allele 1/Allele 2	SD-OCT Category[†]	Foveal Hypoplasia	ELM Ratio		ISe Ratio	
								1 mm	*1.5 mm*	*1 mm*	*1.5 mm*
1	7	M	23.93	*CNGA3*	c.1641C>A-p.Phe547Leu / c.1641C>A-p.Phe547Leu	3	Y	0.32	0.41	1.2	1.16
2	10	M	21.27	*CNGA3*	c.1642G>A-p.Gly548Arg / c.67C>T-p.Arg23Ter	1	Y	0.43	0.38	1.2	1.22
3	11	M	23.43	*CNGA3*	c.485A>T-p.Asp162Val / c.485A>T-p.Asp162Val	1	N	0.75	1.18	1.52	1.71
4	11	F	21.25	*CNGA3*	c.536T>A-p.Val179Asp / c.536T>A-p.Val179Asp	2	N	0.79	1.12	1.19	1.53
5	17	M	22.74	*CNGA3*	c.1001C>T-p.Ser334Phe / c.1360A>T-p.Lys454Ter	3	Y	0.66	0.57	1.68	1.09
6	19	F	22.49	*CNGA3*	c.1694C>T-p.Thr565Met / c.661C>T-p.Arg221Ter	2	N	0.83	0.57	2.25	2.26
7	22	F	23.96	*CNGA3*	c.847C>T-p.Arg283Trp / c.1279C>T-p.Arg427Cys	2	N	0.62	0.92	1.63	1.04
8	22	F	24.58	*CNGA3*	c.848G>A-p.Arg283Gln / c.667C>T-p.Arg223Trp	4	Y	0.66	0.64	1.66	1.73
9	24	M	24.57	*CNGA3*	c.848G>A-p.Arg283Gln / c.667C>T-p.Arg223Trp	2	Y	0.94	0.65	1.88	2
10	25	F	22.77	*CNGA3*	c.1315C>T-p.Arg439Trp / c.1315C>T-p.Arg439Trp	5	N/A	0.76	1.03	1.32	2.24
11	27	F	29.26	*CNGA3*	c.661C>T-p.Arg221Ter / c.661C>T-p.Arg221Ter	3	Y	0.76	0.55	2.33	2.41
12	28	F	25.51	*CNGA3*	c.848G>A-p.Arg283Gln / c.667C>T-p.Arg223Trp	4	Y	0.76	0.79	1.73	1.61
13	29	F	22.40	*CNGA3*	c.661C>T-p.Arg221Ter / c.848G>A-p.Arg283Gln	2	N	0.64	0.88	1.11	2.67
14	31	M	23.18	*CNGA3*	c.848G>A-p.Arg283Gln / c.667C>T-p.Arg223Trp	4	Y	0.54	0.77	1.74	1.59
15	32	F	25.52	*CNGA3*	c.1641C>A-p.Phe547Leu / c.1641C>A-p.Phe547Leu	2	Y	0.61	0.42	1.75	1.15
16	34	F	24.38	*CNGA3*	c.1443-1444insC-p.Ile482His fs*6 / c.1706G>A-p.Arg569His	2	Y	0.55	0.56	1.02	1.21
17	35	M	28.06	*CNGA3*	c.661C>T-p.Arg221Ter / c.848G>A-p.Arg282Gln	2	N	0.52	0.61	1.99	2.67
18	49	F	24.90	*CNGA3*	c.67C>T-p.Arg23Ter / c.67C>T-p.Arg23Ter	4	Y	0.69	0.64	1.84	1.27
19	6	M	21.02	*CNGB3*	c.1148delC-p.Thr383Ile fs*13 / c.1578+1G>A - Splice defect	1	N	0.51	0.73	0.83	1.08
20	11	M	23.63	*CNGB3*	c.1148delC-p.Thr383Ile fs*13 / c.1148delC-p.Thr383Ile fs*13	4	Y	0.73	1.05	1.73	2.06
21	11	F	21.21	*CNGB3*	c.595delG-p.Glu199Ser fs*3 / c.1148delC-p.Thr383Ile fs*13	2	Y	0.57	0.56	1.28	1.73
22	12	F	23.28	*CNGB3*	c.1148delC-p.Thr383Ile fs*13 / c.1006G>T-p.Glu336Ter	3	Y	0.93	0.83	2.07	1.75
23	12	F	22.24	*CNGB3*	c.1148delC-p.Thr383Ile fs*13 / c.1148delC-p.Thr383Ile fs*13	2	Y	0.6	0.49	1.61	1.52
24	13	M	23.42	*CNGB3*	c.595delG-p.Glu199Ser fs*3 / c.1148delC-p.Thr383Ile fs*13	1	N	0.44	0.35	1.28	1.19
25	17	F	22.41	*CNGB3*	c.1148delC-p.Thr383Ile fs*13 / c.1148delC-p.Thr383Ile fs*13	3	N	0.82	0.76	1.16	1.11
26	18	M	23.51	*CNGB3*	c.595delG-p.Glu199Ser fs*3 / c.1148delC-p.Thr383Ile fs*13	4	Y	0.65	0.86	2.04	1.47
27	19	M	22.41	*CNGB3*	c.1148delC-p.Thr383Ile fs*13 / c.1148delC-p.Thr383Ile fs*13	4	Y	1.4	0.57	1.96	1.01
28	23	M	23.67	*CNGB3*	c.1148delC-p.Thr383Ile fs*13 / c.1148delC-p.Thr383Ile fs*13	5	Y	0.62	0.54	1.55	1.59
29	24	M	22.65	*CNGB3*	c.1148delC-p.Thr383Ile fs*13 / c.607-608insT-p.Arg203Leu fs*3	1	N	0.54	0.57	0.8	0.67
30	27	M	22.85	*CNGB3*	c.1148delC-p.Thr383Ile fs*13 / c.1853delC-p.Thr618Ile fs*2	5	N/A	0.48	0.43	2.23	3.91
31	33	F	25.91	*CNGB3*	c.1148delC-p.Thr383Ile fs*13 / c.1148delC-p.Thr383Ile fs*13	2	Y	0.53	0.66	1.12	1.26
32	33	F	20.80	*CNGB3*	c.1148delC-p.Thr383Ile fs*13 / c.1148delC-p.Thr383Ile fs*13	1	N	0.55	0.89	2.18	1.32
33	47	M	24.13	*CNGB3*	c.1148delC-p.Thr383Ile fs*13 / c.1148delC-p.Thr383Ile fs*13	4	N	0.76	0.81	2.34	1.7
34	29	M	22.94	*GNAT2*	c.843-844insAGTC-p.His282Ser fs*11 / c.843-844insAGTC-p.His282Ser fs*11	4	N	0.98	0.93	4.65	4.96
35	43	M	23.55	*GNAT2*	c.843-844insAGTC-p.His282Ser fs*11 / c.843-844insAGTC-p.His282Ser fs*11	1	N	0.74	0.5	2.68	3.15
36	49	F	23.41	*GNAT2*	c.843-844insAGTC-p.His282Ser fs*11 / c.843-844insAGTC-p.His282Ser fs*11	1	N	0.65	0.46	3.47	3.61
37	52	M	24.61	*GNAT2*	c.843-844insAGTC-p.His282Ser fs*11 / c.843-844insAGTC-p.His282Ser fs*11	1	N	0.58	0.64	1.99	2.57
38	43	M	27.45	*PDE6C*	c.304C>T-p.Arg102Trp / c.304C>T-p.Arg102Trp	3	N	0.58	0.87	0.93	2.01
39	19	F	22.28	?	ND	3	Y	0.47	0.55	1.29	1.04
40	23	F	23.05	?	ND	3	Y	0.5	0.48	1.01	1.45

Molecular Genetics

Eighteen subjects (45%) had mutations in *CNGA3* (mean age, 24.1 years; range, 7−49 years), 15 (37.5%) had mutations in *CNGB3* (mean age, 20.4 years; range, 6−47 years), 4 (10%) had mutations in *GNAT2* (mean age, 43.3 years; range, 29−52 years), and 1 subject had a mutation in *PDE6C* (Tables 1, 2, and 4). Seven novel mutations were found in our group of 40 subjects (Table 4). No likely disease-associated variants were identified in 2 individuals, which included screening for *PDE6H* mutations, in addition to these 4 genes. Detailed in silico analysis of both previously described and novel variants is shown in Table 4.[2,19−22]

Foveal Morphology

On the basis of SD-OCT imaging, subjects were placed into 1 of 5 categories (Fig 1): (1) 9 subjects (22.5%) had a continuous ISe layer at the fovea (mean age, 26.8 years; range, 6−52 years); (2) 11 (27.5%) had ISe disruption at the fovea (mean age, 23.8 years; range, 11−35 years); (3) 8 (20%) had an absent ISe layer at the fovea (mean age, 20.6 years; range, 7−43 years); (4) 9 (22.5%) had a foveal HRZ (mean age, 28.2; range, 11−49 years); and (5) 3 subjects (7.5%) had evidence of outer retinal atrophy at the fovea, including RPE loss (mean age, 25 years; range, 23−27 years; Table 5, available at http://aaojournal.org). Of the nine subjects with macular atrophy on fundus examination, 3 subjects were in SD-OCT category 2, 2 in SD-OCT category 3, 1 in SD-OCT category 4, and 3 subjects in SD-OCT category 5. The proportion of subjects with any disruption in cone structure (SD-OCT categories 2−5) was consistent with previous studies.[6−8]

There were no differences in the age ($P = 0.77$), BCVA ($P = 0.44$), contrast sensitivity ($P = 0.57$), or retinal sensitivity ($P = 0.21$) between subjects in the 5 SD-OCT categories; however, reading acuity was significantly worse ($P = 0.02$) in subjects with no ISe disruption compared with subjects with an HRZ (Table 5). Figure 5 shows representative SD-OCT images of subjects of different ages and genotypes, illustrating the variable appearances within different genotypes and the lack of age dependence on the integrity of outer retinal architecture.

Foveal hypoplasia was found in 21 subjects (52.5%) (Table 1; Table 6, available at http://aaojournal.org), with it not being possible to assess hypoplasia in 2 subjects because of severe foveal atrophy. Our rate of hypoplasia was slightly lower than 2 previous reports, which used different definitions of hypoplasia than that used herein.[6,7] There was no significant difference in age, contrast sensitivity, retinal sensitivity, or fixation stability between subjects with or without foveal hypoplasia. Surprisingly, BCVA ($P < 0.01$) and reading acuity ($P < 0.01$) were better in subjects with evidence of foveal hypoplasia compared with those without (Table 6).

ELM and ISe Intensity Ratios

The mean intensity ratios of the ISe band, measured at 1 and 1.5 mm from the fovea in the 40 ACHM subjects, were 1.73 (range, 0.80−4.65) and 1.82 (range, 0.67−4.96), respectively (Table 1). These values were significantly lower compared with 10 controls with mean ISe ratios of 4.26 (range, 1.84−7.81; $P < 0.001$) at 1 mm from the fovea and 3.98 at 1.5 mm (range, 2.01−6.70; $P < 0.001$) from the fovea, although there was overlap between the range of intensity ratios observed in ACHM subjects and controls.

In contrast, the mean intensity ratios of the ELM band, measured at 1 and 1.5 mm from the fovea in the 40 ACHM subjects, were 0.66 (range, 0.32−1.40) and 0.68 (range, 0.35−1.18), respectively (Table 1). These values were similar to those measured in 10 controls, with mean ELM intensity ratios of 0.69 (range, 0.39−1.01; $P = 0.47$) at 1 mm from the fovea and 0.60 at 1.5 mm (range, 0.39−0.84; $P = 0.43$) from the fovea.

No differences were found in ELM or ISe intensity ratios between *CNGA3* and *CNGB3* subjects, with the mean ELM intensity ratios at 1 and 1.5 mm from the fovea being 0.66 and 0.71 in *CNGA3* subjects, and 0.68 and 0.68 in *CNGB3* subjects, respectively ($P = 0.51$ and $P = 0.80$). The mean ISe intensity ratios at 1 and 1.5 mm from the fovea were 1.61 and 1.70 in *CNGA3* subjects, and 1.61 and 1.56 in *CNGB3* subjects, respectively ($P > 0.99$ and $P = 0.32$).

Foveal ONL and Total Retinal Thickness

Mean foveal thickness and ONL thickness at the fovea in ACHM subjects was 163.6 μm (range, 62.0−313.2 μm) and 67.1 μm (range, 26.2−110.5 μm), respectively, which were significantly lower than mean foveal thickness (190.4 μm; range, 136.2−217.0 μm; $P = 0.02$) and mean ONL thickness at the fovea (104.9 μm; range, 82.9−119.5 μm; $P \leq 0.001$) in controls. Again, it is worth noting that there was overlap between the ACHM subjects and controls, consistent with the presence of retained cone nuclei in some ACHM subjects. No correlation was found between age and either foveal thickness ($\rho = 0.03$; $P = 0.84$) or foveal ONL thickness ($\rho = 0.26$; $P = 0.12$) in subjects with ACHM.

Microperimetry

All 40 subjects underwent MP testing on ≥2 occasions. There was no difference in mean retinal sensitivity and fixation stability between eyes, and further analysis was therefore performed using the left eye only in each subject. No difference in mean retinal sensitivity or fixation stability was found between subjects' first and second test; the mean of these 2 tests was used for subsequent analysis.

The mean retinal sensitivity of the group was 16.6 dB (range, 3.1−19.9 dB), and the mean fixation stability of the group was 13.5° (range, 1.7−65°), with significant negative correlations found between retinal sensitivity and (1) age ($\rho = -0.39$; $P = 0.01$; Fig 6), (2) BCVA ($\rho = -0.44$; $P < 0.01$; Fig 7), and (3) reading acuity ($\rho = -0.55$; $P < 0.01$). Surprisingly, a significant correlation was found between lower contrast sensitivity and both higher retinal sensitivity ($\rho = 0.35$; $P = 0.03$) and higher fixation stability ($\rho = -0.43$; $P < 0.01$). There was no difference in mean retinal sensitivity ($P = 0.21$) or fixation stability ($P = 0.34$) across the 5 SD-OCT categories (Table 5). There was a significant correlation between fixation stability and BCVA ($\rho = 0.43$; $P < 0.01$).

Table 1 (cont.)

ELM = external limiting membrane; ISe = inner segment ellipsoid; F = female; M = male; N/A = not possible to assess due to presence of outer retinal atrophy; No = number; ND = no mutation detected; Pt. = patient; SD-OCT = spectral domain optical coherence tomography.
The cDNA is numbered according to Ensembl transcript ID: *CNGA3* ENST00000409937; *CNGB3* ENST00000320005; *GNAT2* ENST00000351050; *PDE6C* ENST00000371447, in which +1 is the A of the translation start codon.
†1 = continuous ISe; 2 = ISe disruption; 3 = ISe absence; 4 = hyporeflective zone; 5 = outer retinal atrophy.

Table 2. Summary of Clinical Characteristics

Variable	Mean (SD)	Range	Median	No. (%)
Age (yr)	24.9 (12.3)	6–52	23.5	—
Visual acuity (logMAR)	0.92 (0.13)	0.72–1.32	0.9	—
Contrast sensitivity (logCS)	1.16 (0.23)	0.50–1.55	1.2	—
Reading acuity (logMAR)	0.76 (0.19)	0.50–1.32	0.73	—
Retinal sensitivity (dB)	16.6 (3.4)	3.1–19.9	17.6	—
BCEA (degrees)	13.5 (13.5)	1.7–65	7.7	—
Genotype				
CNGA3	—	—	—	18 (45)
CNGB3	—	—	—	15 (37.5)
GNAT2	—	—	—	4 (10)
PDE6C	—	—	—	1 (2.5)
Unknown	—	—	—	2 (5)
SD-OCT category*				
1	—	—	—	9 (22.5)
2	—	—	—	11 (27.5)
3	—	—	—	8 (20)
4	—	—	—	9 (22.5)
5	—	—	—	3 (7.5)
Foveal hypoplasia				
No	—	—	—	17 (42.5)
Yes	—	—	—	21 (52.5)
Unrecordable	—	—	—	2 (5)
Fundus appearance category†				
1	—	—	—	11 (28)
2	—	—	—	20 (50)
3	—	—	—	9 (22)

logMAR = logarithm of the minimum angle of resolution; logCS = logarithm of contrast sensitivity; SD = standard deviation; dB = decibels; BCEA = bivariate contour ellipse area; SD-OCT = spectral domain optical coherence tomography; ISe = inner segment ellipsoid; RPE = retinal pigment epithelium.
*SD-OCT category: 1 = continuous ISe; 2 = ISe disruption; 3 = ISe absence; 4 = hyporeflective zone present; 5 = outer retinal atrophy.
†Fundus appearance category: 1 = no RPE disturbance; 2 = RPE disturbance; 3 = Atrophy present.

Six subjects had a scotoma (0 dB sensitivity in ≥1 location), with a mean sensitivity in this group of 11.0 dB (range, 3.1–14.8 dB), and mean fixation stability of 12.8° (range, 1.7–24°). The mean age of these subjects was 40.2 years (range, 25–52 years) and mean BCVA was 1.01 logarithm of the minimum angle of resolution (range, 0.8–1.32). Four of these 6 subjects had RPE disturbance on fundus examination, with the remaining 2 subjects having macular atrophy. It is of note that variable macular structure was seen on SD-OCT, with 3 of the 6 subjects having a normal ISe layer, and 1 subject each having an absent foveal ISe layer, or HRZ, or outer retinal atrophy.

Genotype–Phenotype Correlation

The vast majority (82.5%) of subjects in our study had either *CNGA3* or *CNGB3* mutations. There were no differences between the subjects with these 2 genotypes in terms of age, BCVA, contrast sensitivity, reading acuity, or fixation stability (Table 7, available at http://aaojournal.org). However, retinal sensitivity was significantly greater in the *CNGB3* group than in the *CNGA3* group (18.1 vs 16.1 dB; $P = 0.04$).

A comparison of the SD-OCT phenotypes and presence of foveal hypoplasia failed to identify any consistent differences between the *CNGA3* and *CNGB3* subjects. Specifically, 26.7% of subjects (n = 4) with *CNGB3* mutations had no ISe disruption, compared with 11.1% (n = 2) with *CNGA3* variants; 20% (n = 3) harboring *CNGB3* variants had ISe disruption compared with 44.4% (n = 8) in the *CNGA3* group (Table 7). The presence of an HRZ was similar in *CNGA3* (n = 4; 22.5%) and *CNGB3* (n = 4; 26.7%) subjects. Outer retinal atrophy was observed in 13.3% (n = 2) of *CNGB3* subjects compared with 5.5% (n = 1) of *CNGA3* subjects. In the *CNGA3* group, 61% of subjects (n = 11) had foveal hypoplasia, compared with 53% of *CNGB3* subjects (n = 8). Foveal hypoplasia was not present in the 4 subjects with *GNAT2* mutations or in the single *PDE6C* subject.

On examination, 44.4% of *CNGA3* subjects (n = 7) had a normal fundus appearance, compared with 20% (n = 3) in the *CNGB3* group; 33.3% of *CNGA3* subjects (n = 6) had RPE disturbance compared with 53% of subjects with *CNGB3* variants (n = 8). The percentage of subjects with macular atrophy was similar in both groups (*CNGA3*, 22.3% [n = 4]; *CNGB3*, 27% [n = 4]). Of the 6 subjects with a scotoma on MP, 4 had *GNAT2* variants, 1 had *PDE6C* variants, and 1 had *CNGA3* variants. In addition, BCVA, contrast sensitivity, reading acuity, and mean sensitivity were lower in the *GNAT2* and *PDE6C* genotypes, compared with the *CNGA3* or *CNGB3* groups; however, the mean age of subjects with either *GNAT2* or *PDE6C* mutations was considerably higher than the *CNGA3*/*CNGB3* group (Table 7). Interestingly, 3 out of the 4 subjects with *GNAT2* mutations had an intact ISe layer, despite a relatively low mean retinal sensitivity of 13.6 dB, with all of these subjects having a central scotoma on MP.

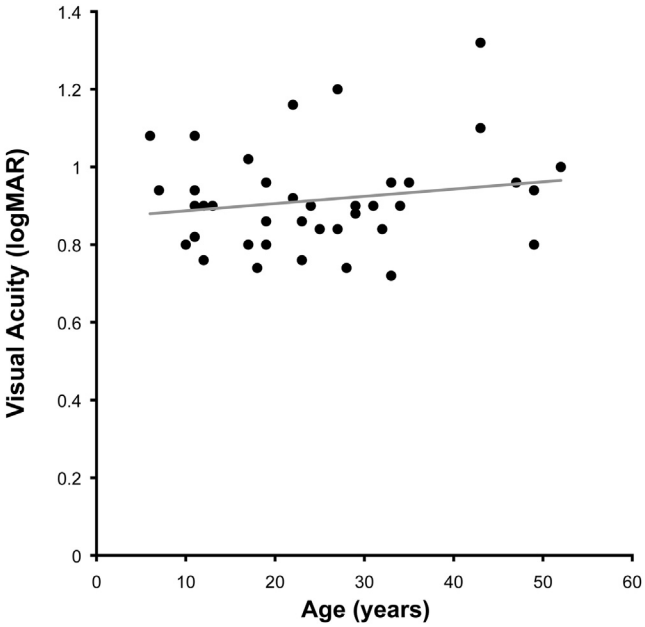

Figure 4. No significant decline in visual acuity as a function of age. Forty subjects with a mean age of 24.9 years (range, 6–52) were included in this study, with a mean visual acuity of 0.92 (range, 0.72–1.32). There was no correlation between age and visual acuity ($r = 0.18$; $P = 0.27$). Acuity reported as logarithm minimum angle of resolution (logMAR).

Discussion

Lack of Age Dependence of Cone Loss

Our cross-sectional study (n = 40) identified no age-dependent loss of cone structure in subjects with ACHM. For example, we found that cone loss (SD-OCT categories

Table 4. Summary of Potentially Disease-Associated Nonsynonymous Sequence Variants Identified in *CNGA3*, *CNGB3*, *GNAT2*, and *PDE6C*

Gene	Nucleotide Alteration	Protein Alteration	Alleles	EVS Observed Allele Count	SIFT Tolerance Index (0–1)	PoyPhen2 HumVar Score (0–1)	Blosum 62 Score (−4 to 11)	Disease Causing	Previously Reported
CNGA3	c.848G>A	p.Arg283Gln	6	A=2/ G=10756	DAMAGING 0.02	PRD 0.996	−1	Yes	Kohl et al 1998[19]
CNGA3	c.661C>T	p.Arg221Ter	5	ND	NA	NA	NA	Yes	Johnson et al 2004[2]
CNGA3	c.667C>T	p.Arg223Trp	4	ND	DAMAGING 0.00	PRD 1.000	−3	Yes	Wissinger et al 2001[20]
CNGA3	c.1641C>A	p.Phe547Leu	4	ND	DAMAGING 0.05	PRD 0.999	0	Yes	Kohl et al 1998[19]
CNGA3	c.67C>T	p.Arg23Ter	3	ND	NA	NA	NA	Yes	Johnson et al 2004[2]
CNGA3	c.485A>T	p.Asp162Val	2	ND	TOLERATED 0.6	POS 0.908	−3	Possibly	Wissinger et al 2001[20]
CNGA3	c.536T>A	p.Val179Asp	2	ND	DAMAGING 0.00	PRD 0.941	−3	Yes	This study
CNGA3	c.1315C>T	p.Arg439Trp	2	ND	DAMAGING 0.01	POS 0.901	−3	Yes	This study
CNGA3	c.1642G>A	p.Gly548Arg	1	ND	DAMAGNG 0.00	PRD 1.000	−2	Yes	Johnson et al 2004[2]
CNGA3	c.847C>T	p.Arg283Trp	1	T=1/ C=10757	DAMAGING 0.00	PRD 1.000	−3	Yes	Kohl et al 1998[19]
CNGA3	c.1001C>T	p.Ser334Phe	1	ND	TOLERATED 1.00	POS 0.744	−2	Possibly	This study
CNGA3	c.1694C>T	p.Thr565Met	1	T=2/ C=13004	DAMAGING 0.03	PRD 0.999	−1	Yes	Wissinger et al 2001[20]
CNGA3	c.1360A>T	p.Lys454Ter	1	ND	NA	NA	NA	Yes	This study
CNGA3	c.1279C>T	p.Arg427Cys	1	T=10/ C=10748	DAMAGING 0.00	PRD 1.000	−3	Yes	Wissinger et al 2001[20]
CNGA3	c.1706G>A	p.Arg569His	1	A=1/ G=13005	DAMAGING 0.00	PRD 0.991	0	Yes	Wissinger et al 2001[20]
CNGA3	c.1443-1444insC	p.Ile482His fs*6	1	ND	NA	NA	NA	Yes	Johnson et al 2004[2]
CNGB3	c.1148delC	p.Thr383Ile fs*13	23	ND	NA	NA	NA	Yes	Kohl et al 2000[21]
CNGB3	c.595delG	p.Glu199Ser fs*3	3	ND	NA	NA	NA	Yes	Johnson et al 2004[2]
CNGB3	c.1006G>T	p.Glu336Ter	1	ND	NA	NA	NA	Yes	Kohl et al 2000[21]
CNGB3	c.607-608insT	p.Arg203Leu fs*3	1	ND	NA	NA	NA	Yes	This study
CNGB3	c.1853delC	p.Thr618Ile fs*2	1	ND	NA	NA	NA	Yes	This study
CNGB3	c.1578+1G>A	Splice defect	1	ND	NA	NA	NA	Yes	Kohl et al 2000[21]
GNAT2	c.843-844insAGTC	p.His282Ser fs*11	8	ND	NA	NA	NA	Yes	Aligianis et al 2002[22]
PDE6C	c.304C>T	p.Arg102Trp	2	ND	DAMAGING 0.00	PRD 0.999	−3	Yes	This study

NA = not applicable; ND = not detected; POS =possibly damaging; PRD = probably damaging.

The predicted biological effect of nonsynonymous variants identified in *CNGA3*, *CNGB3*, *GNAT2* and *PDE6C* were scored for likely pathogenicity using EVS, SIFT, PolyPhen2, and Blosum62. EVS denotes variants in the Exome Variant Server, NHLBI Exome Sequencing Project, Seattle, WA (available from: http://snp.gs.washington.edu/EVS/, accessed April, 2013). SIFT (version 4.0.4; http://sift.jcvi.org/, accessed April, 2013) results are reported to be tolerated if tolerance index ≥0.05 or damaging if tolerance index <0.05. Polyphen-2 (version 2.1 http://genetics.bwh.harvard.edu/pph2/, accessed April, 2013) appraises mutations qualitatively as benign, POS or PRD based on the model's false positive rate. In the Blosum62 (http://www.ncbi.nlm.nih.gov/Class/FieldGuide/BLOSUM62.txt, accessed April, 2013) substitution matrix score, positive numbers indicate a substitution more likely to be tolerated evolutionarily and negative numbers suggest the opposite.

The cDNA is numbered according to Ensembl transcript ID: *CNGA3* ENST00000409937; *CNGB3* ENST00000320005; *GNAT2* ENST00000351050; *PDE6C* ENST00000371447, in which +1 is the A of the translation start codon. Mutations in the coding region of each gene and at intron-exon boundaries are identified.

3–5) was evident in approximately 57% of subjects (16/28) <30 years of age, but in only 33% (4/12) aged >30 years. Moreover, subjects without ISe disruption (most preserved cone structure) had the second greatest mean age of the 5 SD-OCT categories; no reduction in ISe intensity was found with advancing age. In addition, foveal ONL and total retinal thickness was significantly reduced, although we did not find an association between retinal thinning and advancing age. In contrast with our findings, Thiadens et al[6] reported that cone loss occurred in 42% of affected individuals (8/19) who were <30 years of age, with 95% (20/21) >30 years old showing cone loss on SD-OCT.[6] Thomas et al[7] also reported age-dependent ONL thinning.[7] One possible explanation for this discrepancy is the lack of standardization of how cone loss is measured. Moving forward, it will be important to conduct larger studies with molecularly proven subjects in which the same anatomic measures are undertaken.

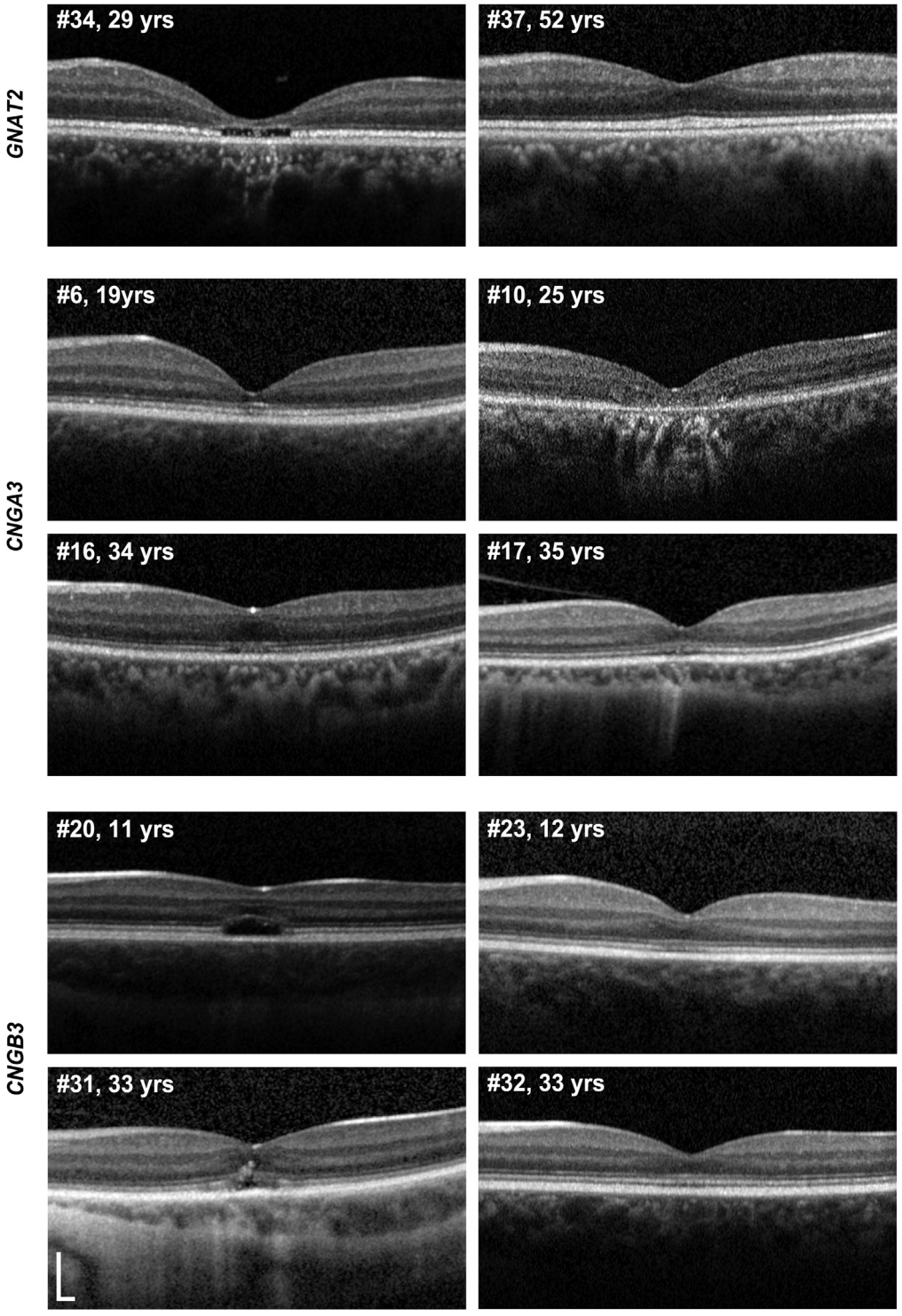

Figure 5. Variable spectral domain optical coherence tomography (SD-OCT) appearance in subjects of various ages and genotypes. Representative SD-OCT images of subjects of different ages and genotypes, illustrating the variable appearances within different genotypes and the lack of age dependence on the integrity of outer retinal architecture.

Although our study demonstrates that outer retinal changes do not necessarily occur in a predictable, age-dependent manner, a recent small (n = 8), longitudinal study observed progressive changes in retinal morphology in younger but not older patients.[23] However, bearing in mind the characteristic phenotypic variability of inherited retinal disease, longitudinal studies are needed to examine the progressive nature of ACHM. It is

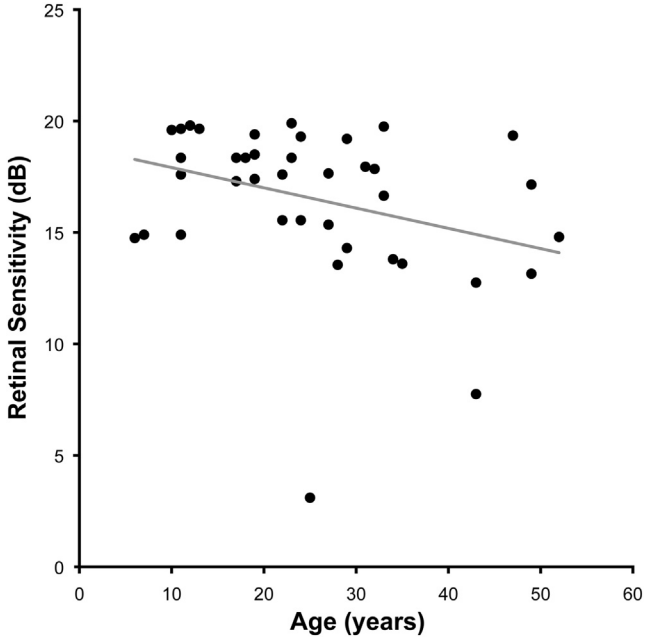

Figure 6. Negative correlation between age and retinal sensitivity. All 40 subjects underwent microperimetry testing on ≥2 occasions. There was no difference in mean retinal sensitivity between both eyes, and further analysis was therefore performed using the left eye only. No difference in mean retinal sensitivity was found between subjects' first and second tests, and the mean of these 2 tests was used for subsequent analysis. The mean retinal sensitivity of the group was 16.6 decibels (range, 3.1−19.9), with significant negative correlation found between retinal sensitivity and age ($\rho = -0.39$; $P = 0.01$). Acuity is reported as logarithm minimum angle of resolution (logMAR). dB = decibels.

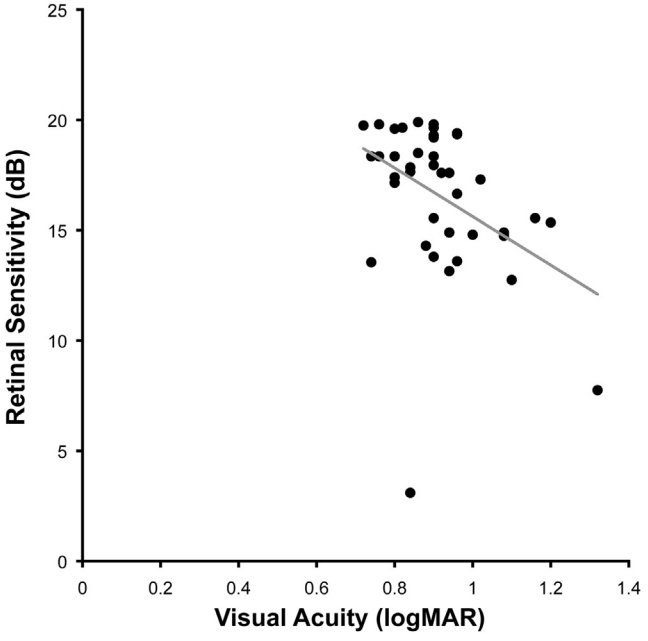

Figure 7. Negative correlation between visual acuity and retinal sensitivity. The mean retinal sensitivity of the cohort was 16.6 decibels (dB) (range, 3.1−19.9 dB) with significant negative correlation found between retinal sensitivity and visual acuity ($\rho = -0.44$; $P < 0.01$). logMAR = logarithm minimum angle of resolution.

important to note that progression does not imply that age alone should be a principal eligibility criterion for emerging trials, as different patients likely progress at different rates.

Retinal Function

We identified no correlation of deterioration in BCVA, contrast sensitivity, or reading acuity with advancing age, and to the best our knowledge, this is the largest study to date reporting any potential change in these parameters with age. We did, however, find a decline in MP-based retinal sensitivity with age. A significant reduction in retinal sensitivity, determined by mesopic MP, has been reported to occur in normal subjects with increasing age, with a 1-dB lower retinal sensitivity found in subjects aged 70 to 75 years compared with those aged 20 to 29 years.[24] In our study, the decline in sensitivity of 3.1 dB observed between subjects <25 years of age (n = 22) and those >25 years old (n = 18) is greater than that potentially attributable to age-related decline.

In our cohort of subjects with absent cone function (on the basis of electrophysiology and psychophysics), it is presumed that retinal sensitivity detected by mesopic MP testing is a consequence of retained rod function. This raises the question as to whether rod function declines in subjects with ACHM with age and if so, why? If there is no change in rod function, it remains a possibility that there is residual central cone function in some subjects, which may deteriorate over time. Further investigation is required to determine which class of photoreceptor(s) is responsible for the retinal sensitivity detected by mesopic MP in ACHM. For example, measuring the rate of recovery of retinal sensitivity using the microperimeter after a full bleach might help to shed light on this intriguing issue.

Structure−Function Relationships

We identified no clear association between retinal structure and function, with no differences in BCVA, contrast sensitivity, retinal sensitivity, or fixation stability between subjects with the various SD-OCT findings or fundus changes. This is in keeping with the lack of an association reported between the presence of an HRZ and visual acuity in previous studies.[6,7] Surprisingly, subjects without ISe disruption had a significantly lower ($P = 0.02$) reading acuity compared with subjects with HRZ presence; however, a statistical difference was not found in any other functional parameter, suggesting this is not a clinically significant observation. No correlation was found between ISe intensity and retinal sensitivity, although this is perhaps to be expected; in the absence of cone function, retinal sensitivity is likely to be primarily derived from rod function in ACHM subjects.

We found no differences in contrast sensitivity, retinal sensitivity, or fixation stability in subjects with or without foveal hypoplasia; however, surprisingly, significantly better BCVA and reading acuity were found in subjects

with foveal hypoplasia. This is reminiscent of findings in albinism, where the absence of a fovea does not necessarily impair acuity.[25,26] However, a structural grading system for foveal hypoplasia reported by Thomas et al[27] has suggested a relationship between foveal development and acuity. It is also likely that varying degrees of nystagmus amplitude or frequency between subjects contribute to determining BCVA and retinal sensitivity in ACHM and other disorders.

Implications for Gene Therapy

Gene replacement trials for both *CNGA3* and *CNGB3* are planned in the near future. Our findings of no age dependence of cone loss demonstrate that the potential window of opportunity for therapeutic intervention in ACHM is wider than has previously been suggested; subjects with no evidence of ISe disruption were aged between 6 and 52 years and we found no correlation of cone photoreceptor disruption or loss with increasing age.

Because this was a cross-sectional study, it has not assessed whether subjects who have any form of outer retinal change develop progressive degeneration, and, if so, how variable the rate of change may be. With respect to cone photoreceptor structure, we therefore suggest that candidates should be considered for potential gene therapy intervention on an individual basis, irrespective of their age. In addition, we did not observe decreased visual function in subjects with foveal hypoplasia; in fact, significantly better BCVA and reading acuity were found in subjects with foveal hypoplasia, suggesting that foveal hypoplasia per se should not be an exclusion criterion for potential therapy trials. In the 9 subjects with no ISe disruption evident on SD-OCT, their mean ISe intensity ratio was considerably lower than in healthy controls, illustrating that assessment of the degree of residual cone structure using this metric may be useful in determining the suitability of potential trial participants. Direct visualization of the cone mosaic is afforded through the use of adaptive optics imaging.[28–30] There is a need to elucidate the relationship between these various measures of cone structure in ACHM to establish the most appropriate means to identify suitable patients and track therapeutic efficacy.

In addition to cone photoreceptor integrity, another factor likely to influence the response to gene therapy is the ability of the visual system to respond to newly acquired input. Functional magnetic resonance imaging has shown evidence of visual cortex reorganization in ACHM subjects, with the area of visual cortex normally active after cone-derived foveal stimulation being active instead after rod stimuli.[31] Conversely, recovery of cone-driven cortical activity has been observed in a canine model of ACHM (Gingras G. Cortical recovery following gene therapy in a canine model of achromatopsia. Paper presented at: The Vision Sciences Society Meeting, May 8, 2009; Florida). The extent to which the visual cortex is able to adapt to and process new input from cone photoreceptors is an additional consideration likely to influence the efficacy of gene replacement therapy.

References

1. Michaelides M, Hunt DM, Moore AT. The cone dysfunction syndromes. Br J Ophthalmol 2004;88:291–7.
2. Johnson S, Michaelides M, Aligianis IA, et al. Achromatopsia caused by novel mutations in both *CNGA3* and *CNGB3* [report online]. J Med Genet 2004;41:e20. Available at:, http://jmg.bmj.com/content/41/2/e20.long. Accessed August 7, 2013.
3. Kohl S, Baumann B, Rosenberg T, et al. Mutations in the cone photoreceptor G-protein alpha-subunit gene *GNAT2* in patients with achromatopsia. Am J Hum Genet 2002;71:422–5.
4. Thiadens AA, den Hollander AI, Roosing S, et al. Homozygosity mapping reveals *PDE6C* mutations in patients with early-onset cone photoreceptor disorders. Am J Hum Genet 2009;85:240–7.
5. Kohl S, Coppieters F, Meire F, et al. European Retinal Disease Consortium. A nonsense mutation in *PDE6H* causes autosomal-recessive incomplete achromatopsia. Am J Hum Genet 2012;91:527–32.
6. Thiadens AA, Somervuo V, van den Born LI, et al. Progressive loss of cones in achromatopsia: an imaging study using spectral-domain optical coherence tomography. Invest Ophthalmol Vis Sci 2010;51:5952–7.
7. Thomas MG, Kumar A, Kohl S, et al. High-resolution in vivo imaging in achromatopsia. Ophthalmology 2011;118:882–7.
8. Genead MA, Fishman GA, Rha J, et al. Photoreceptor structure and function in patients with congenital achromatopsia. Invest Ophthalmol Vis Sci 2011;52:7298–308.
9. Proudlock F, Gottlob I. Foveal development and nystagmus. Ann N Y Acad Sci 2011;1233:292–7.
10. Alexander JJ, Umino Y, Everhart D, et al. Restoration of cone vision in a mouse model of achromatopsia. Nat Med 2007;13:685–7.
11. Michalakis S, Muhlfriedel R, Tanimoto N, et al. Restoration of cone vision in the *CNGA3-/-* mouse model of congenital complete lack of cone photoreceptor function. Mol Ther 2010;18:2057–63.
12. Pang JJ, Alexander J, Lei B, et al. Achromatopsia as a potential candidate for gene therapy. Adv Exp Med Biol 2010;664:639–46.
13. Carvalho LS, Xu J, Pearson RA, et al. Long-term and age-dependent restoration of visual function in a mouse model of *CNGB3*-associated achromatopsia following gene therapy. Hum Mol Genet 2011;20:3161–75.
14. Komaromy AM, Alexander JJ, Rowlan JS, et al. Gene therapy rescues cone function in congenital achromatopsia. Hum Mol Genet 2010;19:2581–93.
15. Hood DC, Zhang X, Ramachandran R, et al. The inner segment/outer segment border seen on optical coherence tomography is less intense in patients with diminished cone function. Invest Ophthalmol Vis Sci 2011;52:9703–9.
16. Huang Y, Cideciyan AV, Papastergiou GI, et al. Relation of optical coherence tomography to microanatomy in normal and *rd* chickens. Invest Ophthalmol Vis Sci 1998;39:2405–16.
17. Spaide RF, Curcio CA. Anatomical correlates to the bands seen in the outer retina by optical coherence tomography: literature review and model. Retina 2011;31:1609–19.
18. Crossland MD, Dunbar HM, Rubin GS. Fixation stability measurement using the MP1 microperimeter. Retina 2009;29:651–6.
19. Kohl S, Marx T, Giddings I, et al. Total colourblindness is caused by mutations in the gene encoding the alpha-subunit of the cone photoreceptor cGMP-gated cation channel. Nat Genet 1998;19:257–9.

20. Wissinger B, Gamer D, Jägle H, et al. *CNGA3* mutations in hereditary cone photoreceptor disorders. Am J Hum Genet 2001;69:722–37.
21. Kohl S, Baumann B, Broghammer M, et al. Mutations in the *CNGB3* gene encoding the beta-subunit of the cone photoreceptor cGMP-gated channel are responsible for achromatopsia (*ACHM3*) linked to chromosome 8q21. Hum Mol Genet 2000;9:2107–16.
22. Aligianis IA, Forshew T, Johnson S, et al. Mapping of a novel locus for achromatopsia (*ACHM4*) to 1p and identification of a germline mutation in the alpha subunit of cone transducin (*GNAT2*). J Med Genet 2002;39:656–60.
23. Thomas MG, McLean RJ, Kohl S, et al. Early signs of longitudinal progressive cone photoreceptor degeneration in achromatopsia. Br J Ophthalmol 2012;96:1232–6.
24. Midena E, Vujosevic S, Cavarzeran F, Microperimetry Study Group. Normal values for fundus perimetry with the microperimeter MP1. Ophthalmology 2010;117:1571–6.
25. Marmor MF, Choi SS, Zawadzki RJ, Werner JS. Visual insignificance of the foveal pit: reassessment of foveal hypoplasia as fovea plana. Arch Ophthalmol 2008;126:907–13.
26. McAllister JT, Dubis AM, Tait DM, et al. Arrested development: high-resolution imaging of foveal morphology in albinism. Vision Res 2010;50:810–7.
27. Thomas MG, Kumar A, Mohammad S, et al. Structural grading of foveal hypoplasia using spectral-domain optical coherence tomography: a predictor of visual acuity? Ophthalmology 2011;118:1653–60.
28. Merino D, Duncan JL, Tiruveedhula P, Roorda A. Observation of cone and rod photoreceptors in normal subjects and patients using a new generation adaptive optics scanning laser ophthalmoscope. Biomed Opt Express [serial online] 2011;2:2189–201. Available at: http://www.opticsinfobase.org/boe/fulltext.cfm?uri=boe-2-8-2392&id=220600. Accessed August 7, 2013.
29. Dubra A, Sulai Y, Norris JL, et al. Noninvasive imaging of the human rod photoreceptor mosaic using a confocal adaptive optics scanning ophthalmoscope. Biomed Opt Express [serial online] 2011;2:1864–76. Available at: http://www.opticsinfobase.org/boe/fulltext.cfm?uri=boe-2-7-1864&id=217386. Accessed August 7, 2013.
30. Carroll J, Dubra A, Gardner JC, et al. The effect of cone opsin mutations on retinal structure and the integrity of the photoreceptor mosaic. Invest Ophthalmol Vis Sci 2012;53:8006–15.
31. Baseler HA, Brewer AA, Sharpe LT, et al. Reorganization of human cortical maps caused by inherited photoreceptor abnormalities. Nat Neurosci 2002;5:364–70.

Footnotes and Financial Disclosures

Originally received: April 13, 2013.
Final revision: August 9, 2013.
Accepted: August 13, 2013.
Available online: October 20, 2013. Manuscript no. 2013-608.

[1] UCL Institute of Ophthalmology, University College London, London, UK.

[2] Moorfields Eye Hospital, London, UK.

[3] Summer Program for Undergraduate Research, Medical College of Wisconsin, Milwaukee, Wisconsin.

[4] Department of Cell Biology, Neurobiology & Anatomy, Medical College of Wisconsin, Milwaukee, Wisconsin.

[5] Department of Ophthalmology, Medical College of Wisconsin, Milwaukee, Wisconsin.

[6] Department of Biophysics, Medical College of Wisconsin, Milwaukee, Wisconsin.

J.C. and M.M. are considered joint senior authors.

Financial Disclosures:
The authors have no proprietary or commercial interest in any of the materials discussed in this article.

Supported by grants from the National Institute for Health Research Biomedical Research Centre at Moorfields Eye Hospital NHS Foundation Trust and UCL Institute of Ophthalmology, Fight for Sight, Moorfields Eye Hospital Special Trustees, The Wellcome Trust, Retinitis Pigmentosa Fighting Blindness, and the Foundation Fighting Blindness (USA). M.M. is supported by a Foundation Fighting Blindness Career Development Award. J.W.B. is an NIHR Research Professor. MCW Funding: NIH grants R01EY017607, P30EY001931, C06RR016511, Foundation Fighting Blindness, and an unrestricted departmental grant from Research to Prevent Blindness (RPB). A.D. is the recipient of a Burroughs Wellcome Fund Career Award at the Scientific interface and a Career Development Award from RPB.

Correspondence:
Michel Michaelides, MD, FRCOphth, UCL Institute of Ophthalmology, 11-43 Bath Street, London, EC1V 9EL, UK. E-mail: michel.michaelides@ucl.ac.uk.